doi:10.1093/plphys/kiab250 PLANT PHYSIOLOGY 2021: 187: 247–262

Plant Physiology®

Research Article

MADS-box transcription factors MADS11 and DAL1 interact to mediate the vegetative-to-reproductive transition in pine

Jing-Jing Ma ,[1] Xi Chen,[1] Yi-Tong Song,[1] Gui-Fang Zhang,[1] Xian-Qing Zhou,[2] Shu-Peng Que,[3] Fei Mao,[3] Tariq Pervaiz,[1] Jin-Xing Lin,[1] Yue Li,[1] Wei Li ,[1] Harry X. Wu ,[1] and Shi-Hui Niu [1,*,†]

1 Beijing Advanced Innovation Center for Tree Breeding by Molecular Design, National Engineering Laboratory for Tree Breeding, College of Biological Sciences and Technology, Beijing Forestry University, Beijing 100083, PR China
2 Qigou State-Owned Forest Farm, Pingquan, Hebei Province 067509, PR China
3 Beijing Ming Tombs Forest Farm, Beijing 102200, PR China
4 Department of Forest Genetics and Plant Physiology, Umeå Plant Science Centre, Swedish University of Agricultural Sciences, Umeå SE-901 83, Sweden

*Author for communication: arrennew@bjfu.edu.cn
†Senior author.

J.J.M. acquired, analyzed, interpreted data, and drafted the manuscript. J.J.M., X.C. and Y.T.S. participated in the sample preparation and performed experiments. G.F.Z., J.X.L., and T.P. provided valuable discussions and helped to refine the draft. X.Q.Z. provided the cultivation and conservation the different age *P. tabuliformis* materials. S.P.Q. and F.M. discovered and identified the *Pinus bungeana* mutant. S.H.N., W.L., Y.L., and H.X.W. participated in the design of the study and performed the statistical analysis. S.H.N. conceived the study and participated in the funding acquisition and project administration, and helped to draft the manuscript. All authors read and approved the final manuscript.
The author responsible for distribution of materials integral to the findings presented in this article in accordance with the policy described in the Instructions for Authors (https://academic.oup.com/plphys/pages/general-instructions) is: Shi-Hui Niu (arrennew@bjfu.edu.cn).

Abstract

The reproductive transition is an important event that is crucial for plant survival and reproduction. Relative to the thorough understanding of the vegetative phase transition in angiosperms, a little is known about this process in perennial conifers. To gain insight into the molecular basis of the regulatory mechanism in conifers, we used temporal dynamic transcriptome analysis with samples from seven different ages of *Pinus tabuliformis* to identify a gene module substantially associated with aging. The results first demonstrated that the phase change in *P. tabuliformis* occurred as an unexpectedly rapid transition rather than a slow, gradual progression. The age-related gene module contains 33 transcription factors and was enriched in genes that belong to the MADS (MCMI, AGAMOUS, DEFICIENS, SRF)-box family, including six *SOC1-like* genes and *DAL1* and *DAL10*. Expression analysis in *P. tabuliformis* and a late-cone-setting *P. bungeana* mutant showed a tight association between *PtMADS11* and reproductive competence. We then confirmed that MADS11 and DAL1 coordinate the aging pathway through physical interaction. Overexpression of *PtMADS11* and *PtDAL1* partially rescued the flowering of *35S::miR156A* and *spl1,2,3,4,5,6* mutants in Arabidopsis (*Arabidopsis thaliana*), but only *PtMADS11* could rescue the flowering of the *ft-10* mutant, suggesting *PtMADS11* and *PtDAL1* play different roles in flowering regulatory networks in Arabidopsis. The *PtMADS11* could not alter the flowering phenotype of *soc1-1-2*, indicating it may function differently from *AtSOC1* in Arabidopsis. In this study, we identified the *MADS11* gene in pine as a regulatory mediator of the juvenile-to-adult transition with functions differentiated from the angiosperm *SOC1*.

Received January 11, 2021. Accepted May 12, 2021. Advance access publication May 29, 2021

Introduction

The irreversible transformation of plants from the vegetative to reproductive phase is referred to as the vegetative phase change (Poethig, 2013) and is a crucial stage in the lifecycle of plants. Prior to beginning reproduction during their long-life cycle, many perennial woody plants experience a prolonged juvenile phase. In the conifer Norway spruce (*Picea abies*), about 20–25 years are required to reach reproductive age (Chalupka and Cecich, 1997), while *Pinus tabuliformis* needs 5–7 years to complete its juvenile phase. Despite considerable progress in the understanding of flowering time control in model plants, such as *Arabidopsis thaliana* (from now on Arabidopsis) and economically important corps, the mechanism underlying the aging pathway in perennial trees, especially conifers, remains largely unclear. Therefore, to explore the effects of aging on the processes of reproductive development in forest trees is of great theoretical and practical importance.

In angiosperms, studies have revealed that an aging pathway mediated mainly by microRNAs (miRNAs) affects the juvenile-to-adult phase transition (Khan et al., 2014); among them, miR156 and miR172 have been identified as key regulatory factors (Lauter, 2005; Wu, 2006;Wu et al., 2009). miR156 and miR172 show evolutionary and expression conservation in annual and perennial angiosperm plants including Arabidopsis (Wu et al., 2009), *Oryza sativa* (Xie, 2006), *Zea mays* (Chucka, 2011), and *Populus* × *canadensis* (Wang et al., 2011). The miR156 accumulates to high levels in seedlings and its expression level gradually decreases during the development of Arabidopsis (Wu, 2006), while miR172 shows the opposite expression pattern (Wu et al., 2009). The expression level of miR156 gradually decreases, resulting in a gradual increase in SQUAMOSA-PROMOTER-BINDING PROTEIN-LIKE (SPL) proteins, after which SPL9 activates miR172 expression (Wang, 2009; Wu et al., 2009). The miR172 continuously inhibits the expression of a small group of *APETALA2-like (AP2-like)* genes, including *AP2*, *TARGET OF EAT1,3* (*TOE1* and *TOE3*), and *SCHLAFMÜTZE* (*SMZ*), eliminating AP2-like protein inhibition over *FLOWERING LOCUS T* (*FT*), *SUPRESSOR OF OVEREXPRESSION OF CONSTANS 1* (*SOC1*), *APETALA1* (*AP1*), and other *MADS-box* genes, allowing plants to shift from vegetative development to reproductive growth (Wang, 2009; Yant et al., 2010; Zhu and Helliwell, 2011). The expression patterns of miR156 and miR172, which strongly correlated with age, are similar in perennial broadleaf trees (Wang et al., 2011), indicating the conservation of this signaling pathway in angiosperms.

The same transcriptional regulation models between miR156 with *SQUAMOSA PROMOTER BINDING PROTEIN (SBP)-box* genes and miR172 with *AP2* homologous genes have been observed in gymnosperms, such as *Ginkgo biloba* (Zhang et al., 2015), Norway spruce, and *Picea glauca* (Shigyo et al., 2006; Nilsson et al., 2007; Guo et al., 2008; Zhang et al., 2019). In *P. tabuliformis*, we confirmed that miR156 and miR172 specifically cut mRNA target sites for *SPL1,2,3* and *AP2* homologous genes; however, the expression pattern of miR156 and its target genes showed no correlation with age (Niu et al., 2015, 2016). In addition to reproductive regulation, miR156 and miR172 are also involved in the regulation of various developmental processes and stress responses, and whether these functions are conserved evolutionarily has not been elucidated. Thus, determining whether miR156 and miR172 play key roles in the vegetative phase transition in gymnosperms is essential.

MADS-box family genes, such as *AP1* and *SOC1*, play critical roles in the aging pathway (Wu et al., 2009; Yant et al., 2010; Zhu and Helliwell, 2011). The *SOC1* gene is a flowering pathway integrator that is widespread among plants and in Arabidopsis connects many flowering signals related to photoperiod, temperature, hormone, and age (Hepworth et al., 2002; Moon et al., 2003; Jungeun, 2010; Jung, 2012). Although *SOC1-like* genes have been isolated from some gymnosperms, including *Gnetum gnemon* (Winter et al., 1999), *P. abies* (Tandre et al., 1995; Uddenberg et al., 2013), and *Pinus radiata* (Walden et al., 1998), and a *SOC1-like* member in *Cryptomeria japonica* functions in accelerating flowering (Katahata et al., 2014), the regulatory mechanism of these genes in gymnosperms remains unclear.

Among *MADS-box* genes, *AGAMOUS-LIKE 6 (AGL6)-like* genes belong to one of the most mysterious and elusive subfamilies, with a variety of expression patterns and functions in different plants (Rijpkema et al., 2009; Li et al., 2010; DuAn et al., 2012; Dreni and Zhang, 2016; Ma et al., 2019). The *AGL6* subfamily, present in both gymnosperms and angiosperms, plays important roles in control of the floral meristem and the production of floral organs and seeds in angiosperms (Rijpkema et al., 2009; Li et al., 2010; Shen et al., 2019). Ectopic expression of *AGL6-like* genes of orchid (*Oncidium Gower*; Hsu et al., 2014) and rice (Li et al., 2010) promoted flowering by activating the *FT* gene and negatively regulating a subset of *FLOWERING LOCUS C (FLC)/MADS AFFECTING FLOWERING* (*FAM*) clade genes in Arabidopsis (Yoo et al., 2011; Hsu et al., 2014). Moreover, studies in *Petunia hybrida*, rice, and maize indicated that *AGL6* have redundant functions with *SEPALATTA (SEP)* (Rijpkema et al., 2009; Thompson et al., 2009; DuAn et al., 2012). Nevertheless, the functions and regulatory mechanism of the *AGL6* subfamily have not yet been fully elucidated in either angiosperms or gymnosperms.

The spruce *DEFICIENS-AGAMOUS-LIKE 1 (DAL1)* gene is a homolog of the *AGL6* subfamily isolated from conifers (Tandre et al., 1995). *DAL1* has been proposed as a possible mediator of phase change, as its expression is stimulated in the mid-juvenile phase and increases with age in Norway spruce (Carlsbecker et al., 2004). The expression of *DAL1* in conifers rises gradually with age, similar to that of miR172 in angiosperms (Carlsbecker et al., 2004; Xiang et al., 2019). In addition, heterologous expression of conifer *DAL1* in Arabidopsis has led to an obvious early flowering phenotypic change, along with adult features such as the development of leaves with predominantly abaxial trichomes (Carlsbecker

et al., 2004; Katahata et al., 2014). The processes triggered by age-related genes have been characterized in conifers mainly based on studies of homologous genes of angiosperms, and the molecular landscape of the aging pathway in conifers has remained largely unexplored.

With long-growth cycles and highly heterozygous genetic backgrounds, the juvenile-to-adult transition in gymnosperms shows much greater complexity than that in angiosperms. To gain further insights into aging pathways in conifers, we screened for a gene module that was significantly associated with aging in *P. tabuliformis* using samples of seven different age classes for temporal dynamic transcriptome analysis. Further analysis of the age-related gene module revealed that the phase change in *P. tabuliformis* did not occur gradually with age, but instead was more rapid than the expected trend. Moreover, *MADS-box* family genes, especially *SOC1-like* genes in the age-related gene module play substantial roles in the juvenile-to-adult transition. Expression–pattern analysis in *P. tabuliformis* and a super-late cone-setting *P. bungeana* mutant confirmed the tight connection between *PtMADS11* and reproductive competence. Genetic assays conducted in wild-type and mutant Arabidopsis verified the differing functions and active sites of *PtDAL1* and *PtMADS11* in regulating floral initiation. In this study, we further elucidated the regulatory mechanism of the reproductive transformation in pine.

Results

A gene module significantly associated with aging in *P. tabuliformis*

Conifers typically have a very long-life cycle in contrast to other model plants, such as Arabidopsis with short lifespans. In conifers, reproductive development occurs after several years. To explore the mystery of the conifer phase transition and reproductive development, we collected samples of *P. tabuliformis* from plants at seven different age stages for temporal dynamic transcriptome sequencing. Through weighted gene coexpression network analysis (WGCNA), we identified a module containing 493 differentially expressed genes that were significantly correlated with age (R^2 = 0.74; Figure 1A and Table S1). The expression patterns of these genes could be divided into two age-related submodules (Figure 1B), including one that was upregulated with age, containing 332 genes (Figure 1C), and the other one consisting of 161 genes that showed age-related decline (Figure 1D). The expression profiles of genes in these two submodules were divided into seven distinct age groups from juvenile to adult. At 5–7 years, a growth phase change occurred, which is consistent with the timing of the reproductive phase in *P. tabuliformis*. The seventh year is when the transformation from juvenile growth to maturity occurs in *P. tabuliformis*. The polynomial model and general linear model were conducted to match the ages of *P. tabuliformis* and gene expressions (Supplemental Figure S1). The result showed that a simple linear model has poor fit over the time in which reproductive competency is obtained, but is better fit by a polynomial model (Supplemental Figure S1). This suggests an attainment of the reproductive phase change that is more rapid than gradual, contrary to what was previously expected (Nilsson and Brunner, 2004; García-López et al., 2014; Khan et al., 2014). The submodule of genes that are downregulated with age likely plays important roles in maintenance of juvenility and vegetative growth, whereas the upregulated submodule is likely a regulatory component of the juvenile-to-adult phase transition in conifers.

The MADS-domain transcription factors PtDAL1 and SOC1-like are key players in the aging module of *P. tabuliformis*

In the age-related module, 33 transcription factors (TFs) were identified that tightly integrated a coexpression network (Figure 2A). Of note, 11 of these 33 TFs belonged to the MADS-box family, making it the most abundant family, including *PtDAL1* and *PtDAL10* (Carlsbecker et al., 2004; Carlsbecker et al., 2003), which have previously been found to play important roles in the reproductive development of conifers (Figure 2A). The *DAL1*, a potential mediator of the juvenile-to-adult transition in Norway spruce, also showed the highest correlation coefficient with age in *P. tabuliformis* (R^2 = 0.86; Supplemental Figure S2). These results indicate that the MADS-domain TFs are key players in the vegetative phase transition of conifers.

Moreover, six out of the seven *SOC1-like* genes (except *PtDAL4*) in *P. tabuliformis* were found in the age-related coexpression module (Supplemental Figure S3), implying that *SOC1-like* genes may play a dominant role in the vegetative to reproductive transformation, which is mediated by an age-related pathway (Figure 2A; Supplemental Figure S3). The expression levels of *PtMADS11,12,13*, *PtDAL3*, and *PtDAL4* were upregulated in older trees as compared to seedlings, while *PtDAL9* and *PtDAL19* showed a decreasing trend. *PtDAL19* was undetectable in 23- and 33-year-old trees. In addition, principal component analysis (PCA) based on the expression of *PtDAL1* and *SOC1-like* genes clearly divided the samples into four age groups (Figure 2B), showing that *PtDAL1* and *SOC1-like* genes could serve as aging marker genes in *P. tabuliformis*.

Among seven *SOC1-like* genes, *PtMADS11* showed a unique expression pattern and the correlation coefficient with age was R^2 = 0.70 (Supplemental Figure S2). *PtMADS11* remained at undetectable levels in juvenile samples without reproductive development, but was suddenly upregulated at 7 years of age and increased with time and developmental status (Figure 2B). The ability to produce cones in *P. tabuliformis* is normally acquired at the age of 7 years, implying that *PtMADS11* may be a primary TF that is closely associated with the age-related initiation of reproductive growth.

To gain further insights into the functions of the seven *SOC1-like* and *PtDAL1* genes, their detailed expression profiles were analyzed in 347 samples from various tissues and

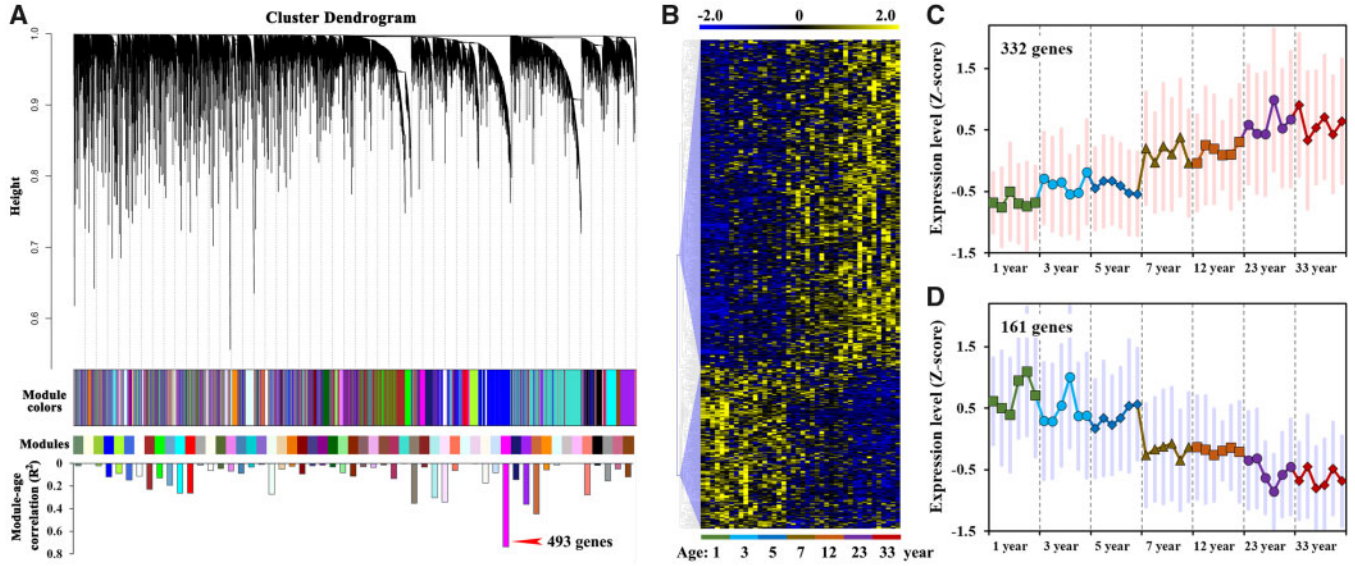

Figure 1 WGCNA and expression patterns of differentially expressed genes from seven different ages. A, WGCNA was conducted on a total of 13,607 genes that were differentially expressed between any two sample groups of the seven different age stages ($P < 0.01$). Six biological replicates (trees) were sequenced for each age group. Based on topological overlap, a cluster dendrogram was produced using gene average linkage hierarchical clustering. Modules of coexpressed genes are shown with different color bars beneath the dendrograms. B, Heatmap of 493 differentially expressed genes that were significantly correlated with age. C, Expression profiles of genes that were upregulated with age. D, Expression patterns of genes that were downregulated with age. The pointes with same shape and color indicate samples in same age group. Each age group represent by six biological replicates (six different trees). The red and blue shading in (C) and (D) represents the maximum and minimum values of all genes in each sample.

age groups of *P. tabuliformis*. As shown in Figure 3 and Supplemental Figure S4, the expression patterns of the seven *SOC1-like* and *PtDAL1* genes were not specific to reproductive development, but also generally accumulated in vegetative organs. High expression of *PtDAL1* was primarily detected in adult shoots as well as female and male cones, whereas low expression was observed in seedling needles, adult roots, and callus (Figure 3). *PtMADS12* showed a similar expression pattern, with high expression levels in adult shoots and female cones, but low levels in juvenile shoots, adult needles and stems, and negligible expression in seedling needles and callus (Supplemental Figure S4). Similarly, *PtMADS13* was expressed at higher levels in adult needles, stems, and shoots. *PtDAL3* was detected primarily in adult stems, with low levels in juvenile shoots, adult needles, adult stems and shoots, male and female cones, and almost undetectable levels in seedling needles, adult roots and callus, in accordance with the general expression profile of *SOC1-like* genes (Supplemental Figure S4). The expression of *PtDAL4* was apparently low in needles but high in shoots of both juvenile and adult trees, but this gene was weakly detected in other tissues (Supplemental Figure S4). Of note, *PtDAL9* was preferentially expressed in seedling needles, but was detected at low levels (barely above background levels) in other samples, and *PtDAL19* was upregulated specifically in juvenile shoots and adult roots (Supplemental Figure S4). *PtDAL9* and *PtDAL19* have been identified in tender and undifferentiated tissues, and the expression profiles of these two genes were distinct from those of the other five *SOC1-like* genes (Supplemental Figure S5). The functions of *SOC1-like* gene family members have been reported to be broad and diversified. The expression of *PtMADS11* followed a strict maturity-related pattern; it was preferentially induced in mature tissues other than roots, and undetectable in any immature organs. Notably, roots are generally considered to maintain a state of continuous division and have a young physiological age (George et al., 2008).

MADS11 is a potential mediator of reproductive ability in conifers

Transformation of conifer species is not possible due to the limited genetic tools available for this group, and functional verification of promising candidate aging pathway genes is extremely difficult. In lieu of such tests, we identified a dwarfed and super-late cone-setting mutant of *Pinus bungeana* from a common garden. The mutant displayed a bushy appearance and shorter needles, a reduced apical dominance and lack of reproductive ability compared to normal *P. bungeana* (Figure 4A; Supplemental Figure S6). *Pinus bungeana* generally transitions to reproductive growth after 10–15 years of vegetative growth, but the mutant had never produced male or female cones at the age of 40 years. We analyzed the expression levels of *PbDAL1* and *SOC1-like* homologs in normal trees and this mutant using RNA sequencing (RNA-seq) and reverse transcription-PCR (RT-PCR) techniques (Table S2). The results showed that *PbMADS11* and *PbDAL3* were not detectable in the mutant, and that the expression of *PbDAL1* and *PbDAL9* was downregulated compared with younger normal trees (Figure 4B). The lack

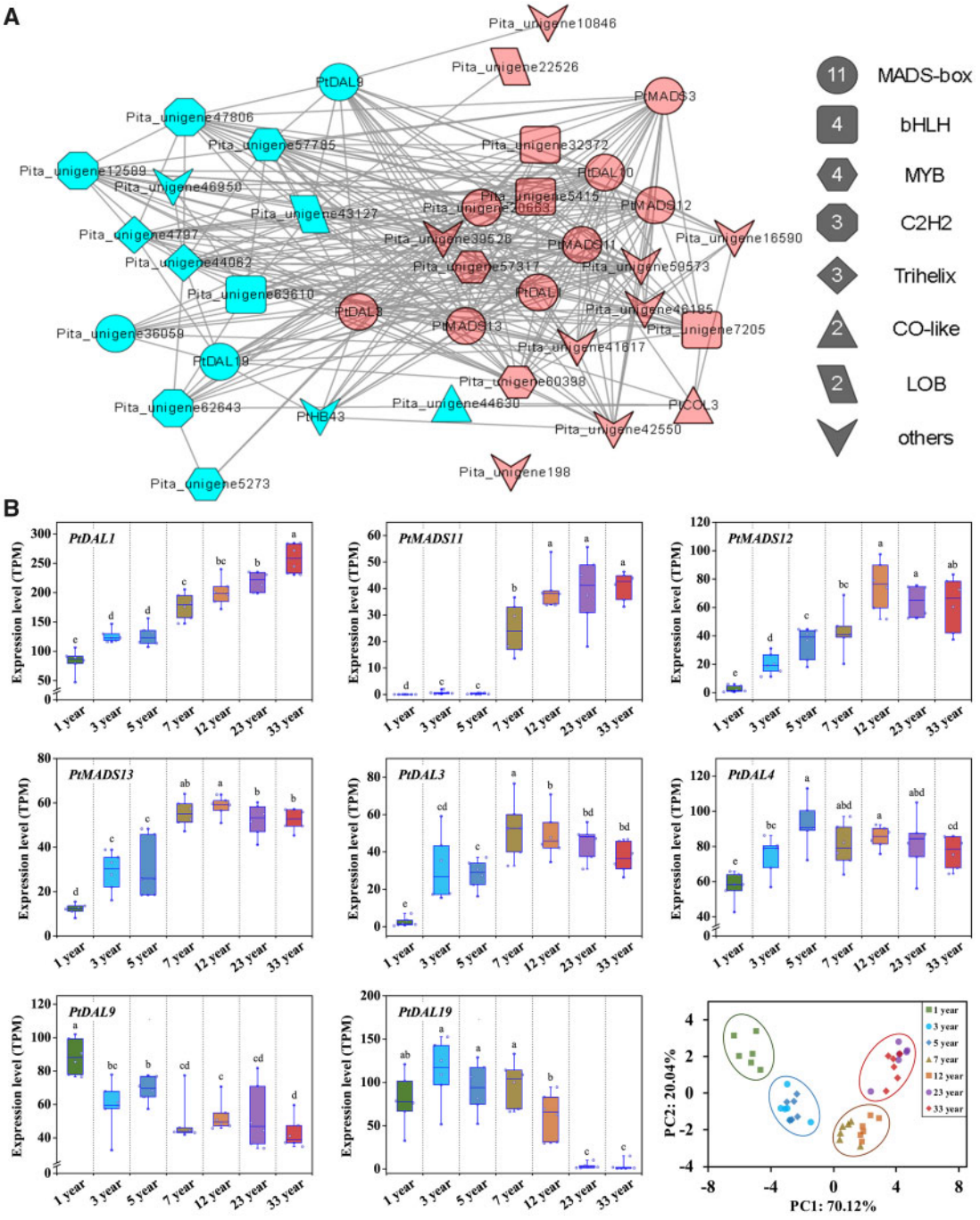

Figure 2 MADS-box TFs are enriched among differentially expressed genes associated with age in *P. tabuliformis*. The coexpression network of 33 tightly integrated TFs. The red shapes represent the genes with expression increase with age, and the blue shapes represent a decrease. B, Expression pattern analysis of *PtDAL1* and seven *SOC1-like* genes in different age groups and PCA for different age groups. The box lower and upper boundaries indicate the 25th and 75th percentiles for each data set. The horizontal lines inside the boxes represent the median values. Whiskers indicate the maximum and minimum values. Different lowercase letters above the plots indicate significant differences at the 0.05 level (ANOVA multiple range test), $n = 6$.

of *PbMADS11* in the *P. bungeana* mutant indicates that *MADS11* may be a mediator of reproductive ability.

In general, coniferous maturation and reproductive ability are assumed to occur in an apical–basal gradient along the tree stem (Hartmann et al., 1997; Carlsbecker et al., 2004). In contrast to basal branches, upper-layer branches generally have greater reproductive ability and typically hold more cones. To further investigate the relationship among *PtDAL1*, *SOC1-like* genes, and reproductive ability, we detected the activities of those genes in six branch whorls from the top toward the base of 15-year-old *P. tabuliformis* through RNA-seq. The apical shoots showed substantially

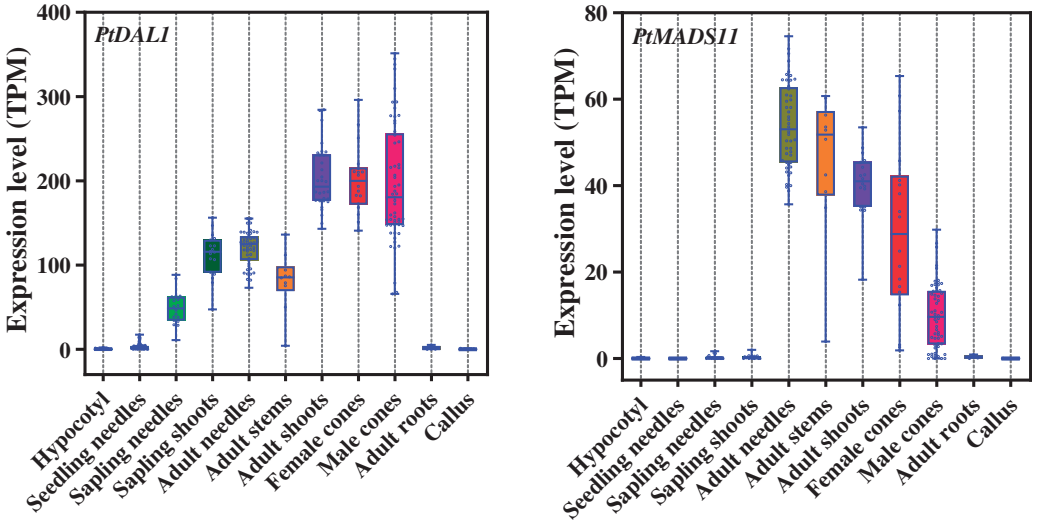

Figure 3 *PtDAL1* and *PtMADS11* expression profiles in various tissues of *P. tabuliformis*. The expression levels of *PtDAL1* and *PtMADS11* in 347 total samples of *P. tabuliformis* were analyzed through RNA-seq, including samples of the hypocotyl (2 months of age, $n = 36$), seedling needles (2 months of age, $n = 90$), sapling needles (3–5 years of age, $n = 18$), sapling shoots (3–5 years of age, $n = 18$), adult needles (33 years of age, $n = 48$), adult stems (33 years of age, $n = 10$), adult shoots (22–33 years of age, $n = 30$), female cones (33 years of age, $n = 18$), male cones (33 years of age, $n = 57$), adult roots (33 years of age, $n = 4$), and callus (induced from the cotyledon, $n = 18$). The lower box and upper boundaries indicate the 25th and 75th percentiles for each data set. The horizontal lines inside the boxes represent the median values. Whiskers indicate the maximum and minimum values.

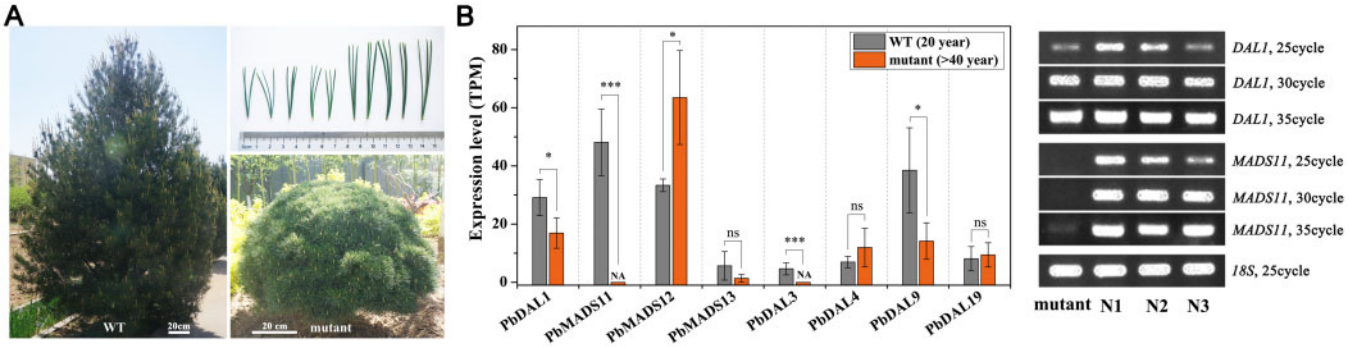

Figure 4 MADS11 is a potential mediator of reproductive ability in conifers. A, Phenotype of the late-cone-setting *P. bungeana* mutant. Normal *P. bungeana* trees grow 3–5 m tall. The *P. bungeana* mutant displayed a dwarfed and bushy appearance. Needle phenotypes of normal (N1–N3) and mutant *P. bungeana*. B, Expression levels of *PbDAL1* and *SOC1-like* homologs in normal and mutant *P. bungeana* trees. The mean of three biological replicates is plotted with SE. *t* test was used to analyze the differences between the two groups of samples. $^{*}P \leqslant 0.05$ and $^{***}P \leqslant 0.001$ between the two groups.

higher expression levels of *PtMADS11*, and expression levels decreased toward the basal part of the tree. The *PtDAL3* also showed spatial patterns along the axis of the tree, but the decreasing trend was not as obvious as that of *PtMADS11* (Supplemental Figure S7). Based on these results, the *PtMADS11* showed a striking relationship with reproductive capacity.

MADS11 and DAL1 coordinate the aging pathway through physical interaction

To investigate the molecular basis of the vegetative to reproductive stage transition regulatory process, a TF collaborative network (TFCN) using an algorithm based on a shared coexpression connectivity matrix (SCCM; Niu et al., 2019) was constructed to screen for hub-coordinated TFs associated with the phase change in conifers. *PtMADS11* and *PtDAL1* showed the highest coordination of TFs among *MADS-box* genes, implying functional coordination (Figure 5A). PtMADS11 and PtDAL1 were both observed in the nucleus and cytoplasm of Arabidopsis protoplasts (Figure 5B). To identify the interaction between PtDAL1 and PtMADS11, yeast two-hybrid (Y2H) assays were performed. Both AD-PtDAL1/BD-PtMADS11 and AD-PtMADS11/BD-PtDAL1 cotransformed yeast strains grew in all dilutions, supporting the role of PtMADS11 as a strong PtDAL1-interacting protein in yeast cells (Figures 5C). Bimolecular fluorescence complementation (BiFC) assays were conducted in *Nicotiana benthamiana* leaves. PtDAL1 was fused with the split N

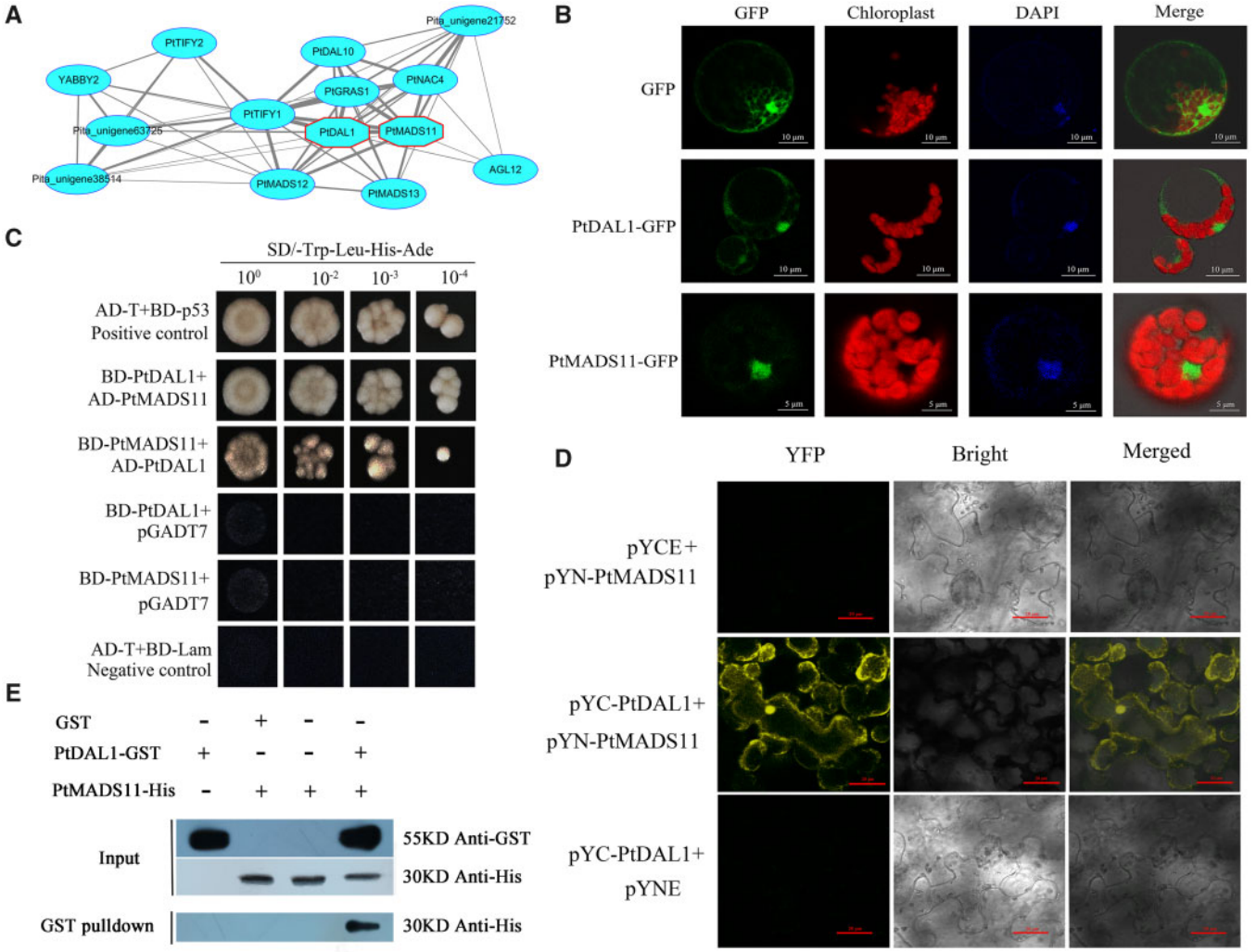

Figure 5 PtMADS11 physically interacts with PtDAL1. A, TFCN based on the SCCM among age-related MADS-box TFs. The red octagons indicate the PtDAL1 and PtMADS11. B, Subcellular localization analysis of PtDAL1 and PtMADS11 performed in Arabidopsis protoplasts. Scale bars: 10 μm (upper two rows) and 5 μm (bottom row). C, Y2H assay of interactions between PtDAL1 and PtMADS11. AD-T and BD-p53 were used as positive control; AD-T and BD-Lam were used as negative control. D, BiFC assay of interactions between PtDAL1 and PtMADS11 in *N. benthamiana* leaf epidermis. YFP, YFP fluorescence; Bright, bright field image; Merge, merged image of YFP and Bright; pYN-PtMADS11, expression of pYN-PtMADS11 alone; pYC-PtDAL1, expression of pYC-PtDAL1 alone; pYN-PtMADS11 + pYC-PtDAL1, coexpression of pYN-PtMADS11 and pYC-PtDAL1. Scale bars: 20 μm. E, GST pull-down analysis of the protein interaction between PtDAL1 and PtMADS11.

terminus of a yellow fluorescent protein (YFP, namely PYN), and PtMADS11 was fused with the split C-terminus of YFP (PYC). When we transiently expressed PYC-PtDAL1 and PYN-PtMADS11, strong YFP signals were observed not only in the nucleus but also in the cytoplasm of leaf epidermal cells (Figure 5D). Moreover, glutathione S-transferase (GST) pull-down assays demonstrated that PtDAL1-GST bound to PtMADS11-His (Figure 5E). Together, these results clearly demonstrate that PtDAL1 and PtMADS11 can form heterodimers through direct protein–protein interaction.

PtMADS11 and PtDAL1 induce early flowering through different mechanisms in Arabidopsis

To elucidate how the *PtDAL1* and *PtMADS11* function in the vegetative phase-change process, *PtDAL1*- and *PtMADS11*-overexpressing transgenic Arabidopsis lines were generated. The transgenic plants displayed visible alterations in morphology from the wild-type, and these improved phenotypic properties were inherited over successive generations. Ectopic expression of the *PtDAL1* gene in wild-type Arabidopsis significantly advanced the phase transition, and the inflorescences reached a height of only 7–9 cm, compared with 30 cm or more for the wild-type (Figure 6A(a); Roberts and Shirsat, 2006). The reproduction of most transgenic plants was initiated considerably after the formation of four rosette leaves bearing abaxial trichomes (Supplemental Figure S8, Aa–d). The geminiflorous organ formed from the fusing of two small carpels and multiple stamens, and the petals were loosely enveloped by four sepals at the top of the inflorescence in transgenic lines (Supplemental Figure S8, Ae–l). The structure formed by the fusion of carpels further developed into two siliques within

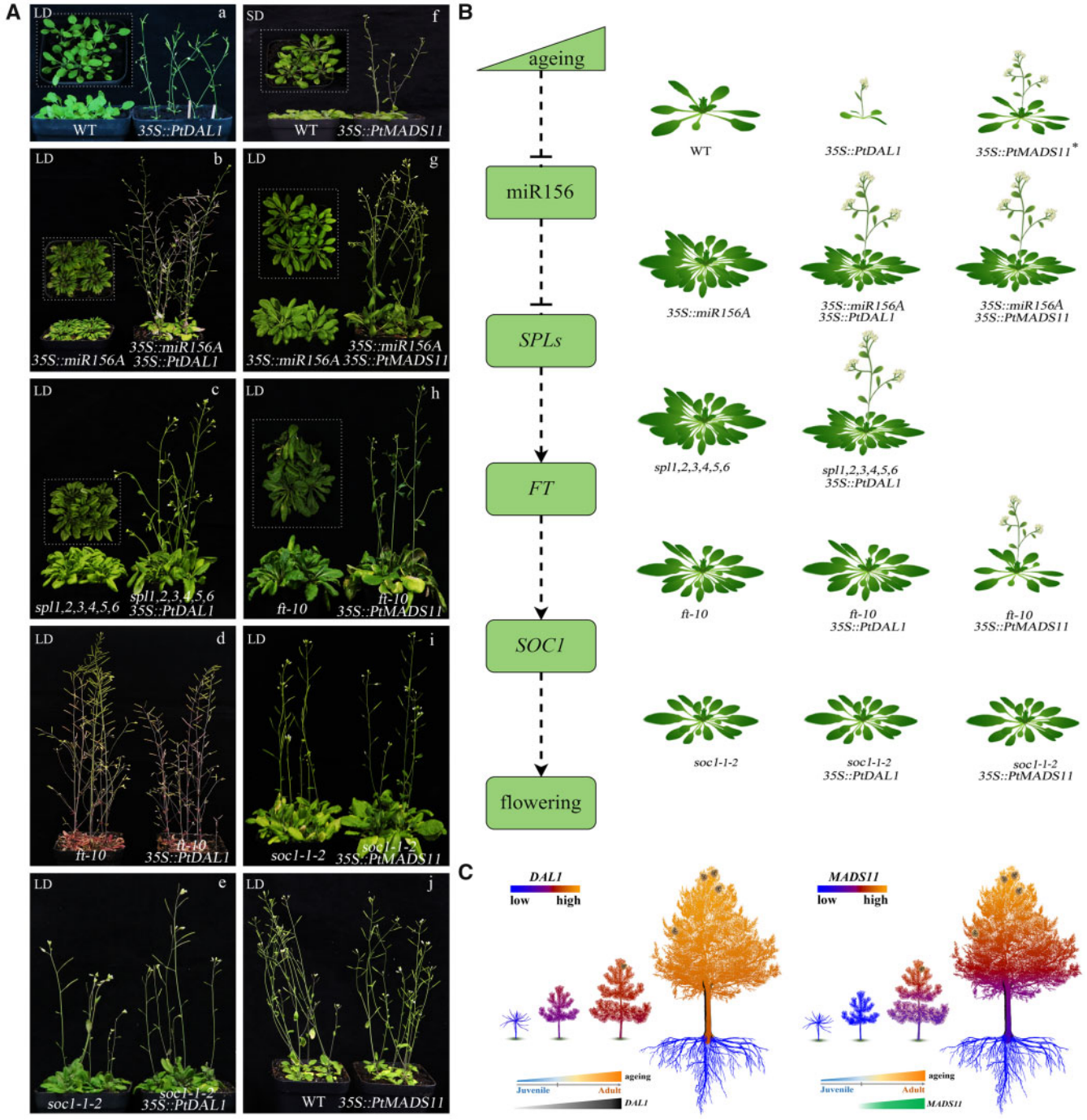

Figure 6 The function of the *PtDAL1* and *PtMADS11* in the flowering regulatory network in Arabidopsis and pine. Transgenic phenotypes of *35S::DAL1* in wild-type and loss-of-function mutant Arabidopsis. a, Ectopic expression of the *PtDAL1* gene significantly advanced the flowering of wild-type Arabidopsis; b, overexpression of *PtDAL1* rescued the late flowering of *35S::miR156A* Arabidopsis lines; c, the late-flowering phenotype of the *spl1,2,3,4,5,6* mutant was restored by overexpression of *PtDAL1*; d, the early flowering phenotype of the *PtDAL1* overexpression lines was suppressed by *ft-10* mutation; e, the overexpression of *35S::PtDAL1* in *soc1-1-2* mutant. f, *35S::PtMADS11* transgenic Arabidopsis exhibited early flowering under SD conditions; g, heterotopic expression of *PtMADS11* restored the severe late-flowering phenotype of *35S::miR156A* Arabidopsis; h, overexpression of *PtMADS11* accelerated flowering with *ft-10* mutation; i, transgenic *PtMADS11* in the *soc1-1-2* mutant caused no apparent alteration in morphology; and j, no obvious phenotypes of overexpression of *35S::MADS11* in wild-type Arabidopsis under LD conditions. The parts of the figure were assembled from more than one photo, and the outlines of each original photo are indicated by dotted lines. B, The model of the *PtDAL1* and *PtMADS11* in the flowering regulatory network of Arabidopsis. *, under SD conditions. C, The expression patterns of *PtDAL1* and *PtMADS11* in *P. tabuliformis* growth process. The red and blue indicate high- and low-expression level, respectively. *PtDAL1* was expressed at low levels in seedlings, and gradually accumulated with age (black triangle). And *PtMADS11* was suddenly activated in tree at 7 years, and then the expression increased with age (green quadrilateral). In adult trees, *PtMADS11* had a downward trend of top-down expression, while *PtDAL1* is relatively consistently expressed between different layer branches. The cones in the trees indicate the reproductive ability of these trees.

one carpopodium (Supplemental Figure S8, C(c)–(e)). In addition to severe phenotypic aberrations in the flowers, oval-shaped cotyledons and curled rosette leaves were produced in the transformants (Supplemental Figure S8Ca). The transgenic plants produced shorter siliques that were often curled and contained fewer seeds compared with those of wild-type plants (Supplemental Figure S8, C(b) and C(f)). These findings confirm the pivotal role of *PtDAL1* in reproductive initiation and control of floral organ identity.

The *35S::PtMADS11* transgenic plants showed early flowering and prematurely terminated inflorescence structures under short-day (SD) conditions, but this flowering promotion effect was greatly attenuated under long-day (LD) conditions (Figure 6, A(f) and A(j)). The loss of inflorescence indeterminacy resulted in production of terminal flowers at the end of the main inflorescence, which then shifted from continuous growth to finite growth (Supplemental Figure S8, B(a)–(h)). Taken together, these results indicate that *PtMADS11* functions as a positive regulator of flowering and a determinant of meristem fate within an inflorescence.

Phenotypic rescue tests were conducted using Arabidopsis mutants defective in key genes of flowering regulatory networks to determine the regulatory mechanism of *PtDAL1* and *PtMADS11* in the phase-transition regulation pathway, as well as their functions in the promotion of flowering in Arabidopsis. Plants overexpressing miR156 and hexamutants of its targets *spl1,2,3,4,5,6* show an extremely severe phenotype of delayed flowering, but the late-flowering phenotype can be restored with overexpression of *PtDAL1*, which allows the transgenic plants to transform normally into the reproductive growth phase (Figure 6, A(b) and A(c)). However, in this study, we found that the early flowering phenotype of *PtDAL1* overexpression lines was suppressed by *ft* loss-of-function mutation (Figure 6A(d)). Similarly, *PtDAL1* did not normalize the phenotype of *soc1-1-2* mutants (Figure 6A(e)). These findings show that the regulatory roles of *PtDAL1* in the reproductive transition are compromised in the absence of either *FT* or *SOC1*. Of note, *fd-3* mutations introduced into the *PtDAL1* gene triggered premature floral development and produced several curly rosettes and cauline leaves (Supplemental Figure S8, D(a)–(c)). Thus, the function of *PtDAL1* in promoting the vegetative phase change in Arabidopsis may be independent of the *FLOWERING LOCUS D* (*FD*) gene. However, heterotopic expression of *PtMADS11* restored the severely late-flowering phenotype of both *35S::miR156A* and *ft-10*, indicating that *PtMADS11* acts independently of miR156 and *FT* in the regulation of flowering (Figure 6, A(g) and A(h)). Similar to *PtDAL1*, *PtMADS11* accumulation had no obvious effect when *SOC1* was absent (Figure 6A(i)). The rosette statistical analysis of transgenic lines was showed in Supplemental Figure S9. Although *PtMADS11* is a *SOC1-like* gene, its function does not overlap with that of *AtSOC1* in Arabidopsis. These results imply that *PtMADS11* and *PtDAL1* play different roles in flowering regulatory networks.

Discussion

There has been considerable progress in understanding flowering time control in model plants such as Arabidopsis (Blumel et al., 2015) and economically important crops such as rice (Yano et al., 2001). However, there are major differences in the regulatory mechanisms of the phase change between conifers and angiosperms (Tandre et al., 1995), and the mechanism underlying the aging pathway in perennial trees, especially conifers, has remained elusive.

In the present study, we identified a gene module that was significantly correlated with aging (Figure 1A). Previous studies suggested that the phase transition in trees occurs gradually (Nilsson and Brunner, 2004; García-López et al., 2014; Khan et al., 2014), but we observed an unexpectedly rapid transition in gene expression from vegetative growth to reproductive development in *P. tabuliformis*. The expression patterns of differentially expressed genes within the age-related module were divided into two age-related submodules (Figure 1B; Supplemental Table S1). The polynomial model and general linear model were further conducted to match the ages with gene expressions (Supplemental Figure S1), which supported our opinion that the phase change in *P. tabuliformis* was a more drastic change than the expected trend. The gene module that was highly correlated with age included two subsets of genes, one of which was upregulated and the other was downregulated as age increased (Figure 1, C and D). In the processes of attaining reproductive competence and reproductive bud differentiation in conifers, up and downregulated gene sets may regulate the balance between vegetative and reproductive growth. A clear understanding of the transcriptional regulation of these up- and downregulated gene sets in the aging pathway will require further research.

In the age-related module, 11 TFs in the MADS-box family accounted for the largest group of the 33 total TFs that tightly integrate a coexpression network (Figure 2A), implying an important role in the reproductive development of conifers. In addition to the MADS-box family, TFs such as MYB, CO-like, and bHLH, which could play roles in the conifer reproductive transformation, were also identified (Figure 2A). In angiosperms, the *CONSTANS* (*CO*) gene functions upstream of the photoperiod pathway and directly regulates the expression of the downstream *FT* gene in leaves to induce flowering (Priyanka and Kishore, 2015; Shim et al., 2017). Several studies on the expression patterns and functions of *CO-like* genes in gymnosperms have suggested that it functions as an inducer that responds to light signals to initiate reproductive growth in gymnosperms (Holefors et al., 2009; Nilsson, 2009; Yan et al., 2017). miR156-targeted *SPLs* negatively regulate the R2R3-MYB–bHLH–WD40 complex to inhibit the expression of anthocyanin biosynthesis genes (An et al., 2012). MYB TFs regulate floral organ differentiation and development in Arabidopsis (Baumann et al., 2007; Zhang et al., 2009). Thus, MYB and bHLH TFs may be involved in the vegetative growth transition in conifers under the control of the aging pathway.

Phylogenetic analyses imply that *SOC1-like* genes in conifers are not orthologs of angiosperm *SOC1-like* genes (Supplemental Figure S3), which derived from the same ancestor and diverged through evolution. After independent functional differentiation of gymnosperm and angiosperm *SOC1-like* genes, a modified cluster consisting of *SOC1-like* genes may act as an integral dominant module that regulates reproduction in gymnosperms, as expression of six *SOC1-like* members of *P. tabuliformis* was tightly correlated with age (Figure 2A). In angiosperms, the *CO* gene positively regulates *SOC1* expression via the *FT* gene in the upstream flowering pathway (Böhlenius, 2006), while *FLC* inhibits *SOC1* expression in the upstream vernalization pathway (Hepworth et al., 2002; Helliwell et al., 2006). The function and mode of action of the *CO* gene in gymnosperms are conserved (Holefors et al., 2009; Nilsson, 2009), but no *FLC* homologs have been found in gymnosperms (Nystedt et al., 2013; Chen et al., 2017). The functions of *SOC1-like* genes in *P. tabuliformis* appeared differentiated within the subcluster due to the presence of two different expression patterns (Supplemental Figure S5). *DAL19* in Norway spruce was specifically upregulated in cone-setting shoots and maintained a high-expression level in adult buds (Uddenberg et al., 2013; Akhter et al., 2018). However, in the present study, *PtDAL19* was undetectable in adult needles, shoots, female cones, and male cones. The opposite expression profiles of *DAL19* between Norway spruce and *P. tabuliformis* reveal the functional differentiation of *DAL19* between Norway spruce and *P. tabuliformis*. Based on large-scale expression data, we propose that *PtMADS11*, *PtDAL3*, *PtDAL4*, *PtMADS13*, and *PtMADS12* predominately promote reproductive growth in the aging pathway, while *PtDAL19* and *PtDAL9* likely act as negative regulators of the juvenile-to-adult phase transition process in *P. tabuliformis*. *SOC1-like* members with opposite functions might share comparable regulatory mechanisms related to age, thereby balancing vegetative growth and reproductive development in *P. tabuliformis*.

Although the expression patterns of *PtDAL1* and *SOC1-like* homologs were strongly correlated with age, expression of these genes was not limited to reproductive organs, and high-expression levels were also detected in vegetative organs (Figure 3; Supplemental Figure S4). Genes such as *FT*, *AP1*, and *LEAFY* (*LFY*), which activate reproductive growth, tend to be activated in vegetative organs, and this feature is conserved among angiosperms (Mandel and Yanofsky, 1995; Moyroud et al., 2010). Moreover, emerging studies have shown that *SOC1-like* genes are involved in a broader range of functions related to enhancing plant tolerance to high temperature and inducing chloroplast biogenesis in petals than previously expected (Wang et al., 2019; Ning et al., 2020). *PtDAL1* and *SOC1-like* homologs may directly sense or transmit signals upstream of age-regulated pathways, with crucial effects on broader network function and reproductive development. The age-mediated response to environmental factors in conifers is worthy of further in-depth investigation.

Expression of *PtMADS11* was almost undetectable in young plants during vegetative growth (1–5 years), and the expression increases after 7 years of growth (Figures 2, B and 6, C). These results imply that *PtMADS11* plays a role in the transformation from vegetative to reproductive growth, and that the seventh year is the end of juvenility in *P. tabuliformis*. The lack of *PbMADS11* in the super-late cone-setting *P. bungeana* mutant supports the close relationship between *MADS11* and reproductive capacity (Figure 4B).

We identified the *DAL1* gene as a primary age biomarker, and it showed the highest correlation coefficient with age (R^2 = 0.86) among the genes investigated in *P. tabuliformis* (Supplemental Figure S2). A transcriptome-wide analysis in *Larix kaempferi* supports the conservation of *DAL1* expression patterns in conifers (Xiang et al., 2019). In contrast to the undetectable expression of *DAL1* in Norway spruce before 5 years (Tandre et al., 1995; Carlsbecker et al., 2004), expression of *PtDAL1* in *P. tabuliformis* was detectable at the seedling stage (Figure 6C). This difference could arise due to the different lengths of the vegetative growth stages of Norway spruce and *P. tabuliformis*. Norway spruce requires 20–25 years before reproducing, while the juvenile phase for *P. tabuliformis* is 5–7 years. *PtDAL1* may function as an activator for shoots to initiate reproduction, but this process may require other coregulators.

In the age-related TFCN module (Figure 5A), beyond *DAL1* and *MADS11*, the *DAL10* gene, which is specifically active in seed cones and pollen cones in Norway spruce, was closely related to reproductive development (Carlsbecker et al., 2003), and *AGL12* was reported to regulate flowering transition in Arabidopsis (Tapia-Lopez et al., 2008). The *GRAS* members functioned on the regulation of phase transition process in barley and rice (Curaba et al., 2013; Fan et al., 2015), and showed an age-related expression pattern in *L. kaempferi* (Xiang et al., 2019). It was also reported that the putative GA-NAC-LFY regulator module might play roles in accelerating reproductive development (Fang et al., 2021). These results confirmed the accuracy of the predicted gene module. The expression of *PtDAL1* increased gradually during the stage of undetectable *PtMADS11* expression (1–5 years) and maintained a higher level than that of *PtMADS11* during the reproductive growth phase (Supplemental Figure S5). In addition, *PtDAL1* had a wider expression range than that of *PtMADS11* among different tissues (Figure 3). The subcellular localization of PtMADS11 protein in cytoplasm and nucleus reasonably explains the interaction between PtDAL1 and PtMADS11 in cytoplasm and nucleus (Figure 5, B and D), which was consistent with MADS-domain protein–protein interactions in Arabidopsis (Immink et al., 2002). These results imply a tight functional coordination between *PtDAL1* and *PMADS11* in an age-mediated module that links the previously expressed regulator *PtDAL1* to the direct interaction factor *PtMADS11* in *P. tabuliformis*. Nevertheless, further evidence is needed to verify the direct regulatory relationship between *PtDAL1* and *PtMADS11*.

PtDAL1 is a homolog of the *AGL6* subfamily in conifers. The *AGL6* subfamily is widespread in plants and has a variety of functions that have been poorly characterized, along with diverse and divergent expression patterns (Reinheimer and Kellogg, 2009 ; Dreni and Zhang, 2016; Ma et al., 2019). The *AtAGL6* is expressed in floral organs and stems in Arabidopsis (Yoo et al., 2011), and two *Gnetum gnemon AGL6* subfamily genes (*GGM9* and *GGM11*) are expressed in both male and female cones, but absent in leaves (Winter et al., 1999; Shen et al., 2019), while *PtDAL1* was detected in the stems, needles, and reproductive cones of *P. tabuliformis* (Figure 3). Despite the divergent expression patterns of the *AGL6* subfamily in plants with distant evolutionary relationships, *AGL6* is generally associated with reproduction (Koo et al., 2010; Callens et al., 2018) and cone formation (Winter et al., 1999). The orchid *AGL6* homolog *OMDS1*, when overexpressed in Arabidopsis, causes an early flowering phenotype by inducing expression of *SOC1*, *FT*, *LFY*, and *AP1* genes (Hsu et al., 2003). This phenotypic similarity in transgenic plants indicates that *DAL1* may have conserved regulatory mechanisms. As a member of the MADS-domain family, AGL6 appears to form multimers with other TFs, which have various interactions with SQUA/AP1-like and AGL proteins (Ma et al., 2019), and to integrate signals at the core of the regulatory network. In conifers, DAL1 is a key node of the aging pathway that can form heterodimers with MADS11 and integrates signals to initiate the juvenile-to-adult transition process.

Ectopic expression of *PtDAL1* led to an extremely early flowering in Arabidopsis (Figure 6A(a)), indicating that this gene plays a dominant role in the initiation of reproductive growth. These results are consistent with those reported in Norway spruce (Carlsbecker et al., 2004). However, the phenotypic changes caused by transformation of genes from conifers into Arabidopsis did not elucidate the underlying mechanism. High expression levels of a number of other *MADS-box* family genes caused early flowering, including *DAL2* and *DAL10* from spruce (Tandre et al., 1998; Carlsbecker et al., 2003), but the effects of *DAL1* on flowering time were more severe than those of other *MADS-box* genes (Carlsbecker et al., 2004), and its effect on the growth of Arabidopsis was particularly strong. The formation of the geminiflorous organ from two short carpels in the *35S::PtDAL1* transgenic lines implied its broader functional roles in floral organ identity and flower development.

During the transition from vegetative growth to flowering in Arabidopsis, *SOC1* had upregulated expression in the apical meristem, which effectively promoted early flowering (Lee et al., 2000; Samach, 2000). The expression level of *CO* increased under LD conditions, which promoted expression of the *FT* gene and then the *SOC1* gene (Yoo et al., 2005). Transgenic *PtMADS11* plants showed no apparent alteration under LD conditions, but exhibited early flowering along with premature termination of inflorescence under SD conditions (Figure 6, A(f) and A(j)). *PtMADS11* may require a positive factor to promote its function in Arabidopsis under SD conditions. Under SD conditions, the Arabidopsis growth cycle was prolonged and the wild-type Arabidopsis contained about 26 rosette leaves compared with 14 rosette leaves under LD conditions (Supplemental Figure S9). The SD conditions extended the period in which *PtMADS11* could play its role and thereby intensified its flowering promotion.

Genetic assays were conducted to verify the functional difference between *PtDAL1* and *PtMADS11* (Figure 6B), as the flowering regulatory network in Arabidopsis has been extensively studied (Blumel et al., 2015). The extremely severe delayed flowering phenotype of *35S::miR156A* lines could be rescued with constitutive expression of *PtDAL1* or *PtMADS11*, implying that the target loci of both transgenic *PtDAL1* and *PtMADS11* were downstream of miR156. The early flowering phenotype of *PtDAL1*-overexpression lines was suppressed by the *ft* loss-of-function mutation, while *ft-10* mutant lines that expressed *35S::PtMADS11* had accelerated flowering (Figure 6, A(d) and A(h)). Theoretically, as an upstream regulator of *FT*, *PtDAL1*, and *PtMADS11* functioned on different positions of the regulatory network in Arabidopsis. Of note, *fd-3* mutations introduced into the *PtDAL1* gene triggered premature floral development, which revealed that the function of *PtDAL1* in promoting flowering in Arabidopsis may be independent of the *FD* gene. In Arabidopsis, *35S::FT* partially rescued the late-flowering phenotype of *fd-1* mutants (Abe et al., 2005), indicating that an FD-independent flowering time regulation pathway exists. Notably, all of the gymnosperm SOC1-like proteins queried nested in a clade outside of the Arabidopsis SOC1 and FLC clade proteins (Supplemental Figure S3), indicating their functions may have differentiated during the evolution (Uddenberg et al., 2013). In the present study, we revealed that *PtMADS11* cannot restore the late-flowering phenotype of *soc1-1-2* mutants; this result suggests that the gymnosperm *SOC1-like* genes probably cannot replace the *SOC1* in Arabidopsis. The differentiated functions of *PtMADS11* support a specific regulatory role in the conifer aging pathway.

In this study, we determined that the phase change in pine was a more rapid change than the expected trend. In total, 33 tightly coordinated TFs were identified from the age-related gene module, among which *SOC1-like* genes were enriched. Among *SOC1-like* homologs, two distinct expression patterns represented two internal submodules with opposite functions, which together could balance vegetative growth and reproductive growth. In this study, we confirmed the function of *PtDAL1* as a regulator in phase transition and identified an interacting gene, *PtMADS11*, which may function as a positive regulator of reproductive capacity in *P. tabuliformis*. The differing active sites of *PtDAL1* and *PtMADS11* were validated through genetic analysis. The results confirm that the functions of *PtDAL1* and *PtMADS11* differ, and that *PtMADS11* may play a unique role in the aging pathway in conifers. Our findings provide a basis for further in-depth studies into the specific regulatory relationships between *DAL1* and *MADS11* in conifers using

more advanced plant genetic engineering tools, such as carbon nanotube carriers.

Materials and methods

Plant materials

For the different ages of *P. tabuliformis* Carr., plants were selected from a primary clonal seed orchard located in Pingquan City, Hebei Province, China (118°44.6758′ E, 40°98.8784′ N, 560–580 m above sea level). Vegetative shoot apexes were collected from the top branches of the trees after bud-break on 10 May 2016. Six different trees were used as biological replicates for RNA-seq analysis. For tissue specific expression analysis, we collected the needles and hypocotyl from *P. tabuliformis* seedlings that were cultured in control conditions (24°C, 16 h for light and 8 h for dark), and the sapling needles and shoots were sampled from 3-year-old trees. The callus was induced from seedling hypocotyls following the published method, and propagated for several generations (Liu et al., 2020). Adult tissue samples, including needles, shoots, stems, cones, and roots, were collected from the same primary clonal seed orchard on 10 May 2016. The mutant of *P. bungeana* was found in a common garden of Beijing Ming Tombs Forest Farm, Beijing, China. Three normal *P. bungeana* trees were selected as controls for gene expression analysis. From six apical to base whorls of branches of three 15-year-old trees in the same primary seed orchard, vegetative shoots of each whorl have been collected on 11 May 2019 and stored at −80 °C for total RNA extraction. All the samples were collected between 12:00 and 13:00 to control the influence of photoperiod during sampling.

All the mutants and transgenic lines of Arabidopsis used in this study were obtained from The Arabidopsis Information Resource (http://arabidopsis.org). The *35::miR156A* transgenic lines prolonged the expression of juvenile vegetative traits and delayed flowering (Wu and Poethig, 2006). The *spl1,2,3,4,5,6* mutant that functioned in delaying vegetative phase change and increasing rate of leaf initiation delayed flowering time equal to *35S::miR156A* (Xu et al., 2016). The *ft-10* mutant displayed a late flowering phenotype under LD conditions (Yoo et al., 2005). The *fd-3* mutant displayed a late flowering phenotype that was unaffected by vernalization, and an increased number of rosette leaves (Koornneef et al., 1991). And the *soc1-1-2* mutant delayed flowering both in LD and SD growth conditions (Lee et al., 2000).

RNA-seq analysis

Total RNA from different samples of *P. tabuliformis* were extracted by the Trizol method (Invitrogen, CA, USA). The cleaved RNA fragments were then reverse-transcribed to create the final complementary DNA (cDNA) libraries using the mRNA-Seq sample preparation kit (Illumina, Inc., San Diego, CA, USA). The cDNA libraries were sequenced on the Illumina NovaSeq platform by using the paired-end module (2 × 150 bp). Clean reads for each sample were aligned to the *P. tabuliformis* reference transcriptome (Niu et al., 2013). Sleuth software was used to analyze differential expression of the genes (Pimentel et al., 2017). The heatmap of the expression cluster of differential genes was analyzed and displayed by Multiple array viewer software. The gene expression patterns of the samples from different conditions were calculated and normalized by the *Z*-score transformation (Cheadle et al., 2003). The coding sequences of *SOC1-like* homologs and *PtDAL1* were available in Supplemental Data Set S1.

Phylogenetic analysis

Multiple alignments of protein sequences were obtained by MAFFT tool (Katoh and Standley, 2013) and the maximum likelihood tree based on the JTT model was obtained using MEGA software (Sohpal *et al.*, 2010). Bootstrap values were obtained by 1,000 bootstrap replicates.

Network construction

The WGCNA was performed on all the samples using the standard method (Zhang and Horvath, 2005; Horvath, 2008). On the basis of topological overlap, a cluster dendrogram was produced by evaluating the average linkage hierarchical clustering of genes. The correlation between module eigengenes and the aging was analyzed. We then chose the module that was most significantly correlated with age for further analysis in the coexpression network.

The TFCN was further constructed using an algorithm based on the SCCM (Nie et al., 2011; Niu et al., 2019). We considered two TFs to be collaborative and connected in the TFCN only if they shared at least 40 coexpressed genes in common from the top 200 most tightly coexpressed genes for each TF.

Subcellular localization analysis

For subcellular localization analysis, 35S::PtDAL1–GFP and 35S::PtMADS11–GFP fusions were constructed under the control of the constitutive 35S promoter with the green fluorescent protein (GFP) coding region. The rosette leaves of Arabidopsis growing for 3–4 weeks under LD conditions (16-h light/8-h dark, 23°C) were cutoff for enzymatic hydrolysate at 22°C for 2 h in dark (Wu et al., 2009). An equal volume W5 solution was added, shaken gently, and the protoplasts were filtered into the new tube by 100 mesh cell sieves. The protoplasts were collected after centrifugation at 150 rpm at room temperature for 2 min. The supernatant was carefully removed and the protoplast was resuspended by adding an appropriate amount of precooled MMG solution. The 35S::PtDAL1-GFP and 35S::PtMADS11-GFP plasmids were each added into 100 μL protoplasts and lightly mixed. Then 110 μL PEG4000 solution was added and incubated at room temperature for 15 min. A 440-μL W5 solution was added to gently terminate the transfection process. The protoplasts were collected after centrifugation at 150 rpm for 2 min and 400-μL WI solution was added. The solution was incubated at 22°C in dark for 16–24 h. After removing the WI solution, DAPI staining solution (5 μg/mL)

was added to cover the protoplasts for 10 min and phosphate-buffered saline (PBS) solution was used to wash the protoplasts three times. The GFP signal was observed by confocal microscope (Leica SP8), the excitation wavelengths and emission filters sets were as 488 nm (Ex)/BP505 to 530 nm (Em). Image analysis was conducted with the Leica LAS AF software.

BiFC assay

For BiFC assays, full-length PtDAL1 and PtMADS11 were cloned into pYCE and pYNE vectors containing the C- or N-terminal end of YFP. The constructs (pYC-PtDAL1 and pYN-PtMADS11) and corresponding empty vectors were each transformed into *Agrobacterium* strain *GV3101-psoup*, then the culture was shaken in a constant temperature shaker for 12–18 h until OD_{600} = 0.6. The bacterial liquid was collected after centrifugation at a room temperature and resuspended with infection solution (10 mM MES, 150 μM AS, 10 mM $MgCl_2$) keeping OD_{600} = 1.0 and pH = 5.6. Then we added 20 μL AS to the bacteria solution and let it stay in the dark for 2–3 h at a room temperature. The two strains of bacteria liquid were mixed and injected into *N. benthamiana* leaves by sterile syringes with the needle removed. During the injection, the blade face of leaves was held with fingers to help the bacteria liquid insinuate the leaves slowly. A small wound could be made by the needle hub to ensure the injection would go smoothly. The inoculated *N. benthamiana* was treated under dark conditions for 24 h, and the fluorescence signal was observed after growth under normal conditions for 48 h (16-h light/8-h dark, 23°C). Fluorescence was then observed by confocal microscope (Leica-SP8), the excitation wavelengths and emission filters sets were 514 nm (Ex)/BP525 to 550 nm (Em). Image analysis was conducted with the Leica LAS AF software.

Y2H assay

Y2H assay was performed to investigate the protein–protein interactions following the Yeast Protocols Handbook (Clontech). The full coding regions of PtDAL1 and PtMADS11 were fused with pGADT7 and pGBKT7 vectors. These constructs and empty vectors as control were then transformed into the Y2H gold yeast strain by the lithium acetate method. The yeast cells cotransformed with plasmids encoding two tested proteins were plated onto selective medium (lacking leucine, tryptophan, histidine, and adenine), and supplemented with aureobasidin A for screening of possible interactions.

GST pull down

Bacteria with overexpressed PtDAL1-GST and PtMADS11-His proteins were resuspended in 20 mM Tris–HCl buffer (pH = 7.5) that contained 0.2 mM EDTA, 0.5 mM dithiothreitol, 0.15 M NaCl, 4 mM benzamidine, and 0.02% NaN_3, and ruptured using a French press. The GST and PtDAL1-GST proteins were adsorbed onto the completely resuspended immobilized glutathione during incubation for 4 h with rotation. After adding PtMADS11-His protein to the glutathione-Sepharose beads, the GST–fusion protein complex was rotated during an overnight incubation under 4°C conditions. The protein complex was centrifuged, the supernatant discarded, and the proteins resuspended in 500 μL PBS (1,250 rpm, 5 min). Then, 100 μL of eluent buffer (20 mM Tris–HCl, pH = 7.5) was used to separate the supernatant from the protein precipitates (30 min, 4°C). The precipitates were analyzed through western blotting. Western blot detection was performed as described previously with minor modifications (Gibbons, 2014).

Plasmid construction and transformation of *A. thaliana*

The *PtDAL1* and *PtMADS11* genes were amplified from the cDNA of *P. tabuliformis* new shoot by PCR using primers that introduced *Xba*I and *Xho*I restriction sites (Supplemental Table S2). The CDS of *PtDAL1* and *PtMADS11* each recombined into the plant expression vector pBI121, which contained the *npt*II gene as a selectable marker, with the 35S promoter. Constructs were transformed into *Agrobacterium* strain *GV3101*, and *35S::PtDAL1* and *35S::PtMADS11* overexpression transgenic Arabidopsis lines were generated by the floral-dip process (Clough and Bent, 1998). All the experiments on Arabidopsis mutants, transgenic lines, and wild-type were conducted with transgenic *35S::PtDAL1* and *35S::PtMADS11* to determine their functions in the flowering regulatory network. The harvested seeds were screened on MS mediums containing Kanamycin antibiotic (50 $mg \cdot mL^{-1}$) until homozygous lines were obtained. All of the Arabidopsis plants were grown in an artificial climate box under LD conditions (16-h light/8-h dark, 23°C) or SD conditions (8-h light/16-h dark, 23°C). The transgenic Arabidopsis lines used in this study were shown in Supplemental Table S3. Nine transgenic lines for each experiment were randomly selected, and at least 30 events were counted for rosette leaf number statistics. The significance of differences between transgenic lines and mutants or wild-type Arabidopsis was analyzed by *t* test.

Data availability

The authors declare that all data supporting the findings of this study are available within the article and Supplementary Material online or are available upon request from the corresponding author. The RNA-seq data that support the findings of this study have been deposited in the CNSA (https://db.cngb.org/cnsa/) of China National GeneBank Database with accession number CNP0001648.

Accession numbers

The accession numbers of Arabidopsis mutants mentioned in this article are as follows: CS69799 (*spl10-3*; *spl11-1*; *spl13-1*; *spl15-1*; *spl2-1*; *spl9-4*); CS67849 (*35S::miR156A*); SALK_054421C (*fd-3*); SALK_006054C (*soc1-1-2*); and CS9869 (*ft-10*).

Supplemental data

The following materials are available in the online version of this article.

Supplemental Figure S1. The polynomial model (R^2 = 0.86) and general linear model (R^2 = 0.74) of the expression level of 493 differential genes matching age stages in *P. tabuliformis*.

Supplemental Figure S2. The correlation coefficient of age with the expression level of *PtDAL1* and *PtMADS11*.

Supplemental Figure S3. The phylogenetic tree of SOC1-like proteins in Arabidopsis and *P. tabuliformis*.

Supplemental Figure S4. The expression patterns of *SOC1-like* genes except *PtMADS11* expression during aging in *P. tabuliformis*.

Supplemental Figure S5. The *PtDAL1* and *SOC1-like* genes expression pattern during aging in *P. tabuliformis*.

Supplemental Figure S6. The silhouettes of dwarf mutant and normal *P. bungeana* at the same scale.

Supplemental Figure S7. Expression profiles of *PtDAL1* and seven *SOC1-like* homologs in six branch whorls from top to base of 15-year-old *P. tabuliformis*.

Supplemental Figure S8. The phenotype of *35S::PtDAL1* transgenic Arabidopsis lines.

Supplemental Figure S9. Analysis of rosette leaf number at flowering of Arabidopsis transgenic and mutant lines.

Supplemental Table S1. A list of all 493 differentially expressed genes of *P. tabuliformis* among different ages.

Supplemental Table S2. Primers used for plasmid construction RT-PCR analysis.

Supplemental Table S3. The transgenic Arabidopsis lines used in this study.

Supplemental Dataset S1. The coding sequences of *SOC1-like* homologs and *PtDAL1* in *P. tabuliformis*.

Acknowledgments

We would like to thank Meiqin Liu and the Testing and Analysis Center of Beijing Forestry University for the help with confocal microscopy. We would like to thank Dongmei Hu for her help in drawing the diagram.

Funding

This work was supported by The National Natural Science Foundation of China (grant no. 31870651), National Key R&D Program of China (grant no. 2017YFD0600500), and The Program of Introducing Talents of Discipline to Universities (111 project, B13007).

Conflict of interest statement. The authors declare that they have no conflicts of interest.

References

Abe M, Kobayashi Y, Yamamoto S, Daimon Y, Yamaguchi A, Ikeda Y, et al. (2005) FD, a bZIP protein mediating signals from the floral pathway integrator *FT* at the shoot apex. Science **309**: 1052–1056

Akhter S, Kretzschmar WW, Nordal V, Delhomme N, Street NR, Nilsson O, et al. (2018) Integrative analysis of three RNA sequencing methods identifies mutually exclusive exons of MADS-box isoforms during early bud development in *Picea abies*. Front Plant Sci **9**: 1625

An X, Tian Y, Chen K, Wang X, Hao Y (2012) The apple WD40 protein MdTTG1 interacts with bHLH but not MYB proteins to regulate anthocyanin accumulation. J Plant Physiol **169**: 710–717

Baumann K, Perez-Rodriguez M, Bradley D, Venail J, Bailey P, Jin H, et al. (2007) Control of cell and petal morphogenesis by R2R3 MYB transcription factors. Development **134**: 1691–1701

Blumel M, Dally N, Jung C (2015) Flowering time regulation in crops-what did we learn from Arabidopsis? Curr Opin Biotechnol **32**: 121–129

Callens C, Tucker MR, Zhang D, Wilson ZA (2018) Dissecting the role of *MADS-box* genes in monocot floral development and diversity. J Exp Bot **69**: 2435–2459

Carlsbecker A, Sundstrom J, Tandre K, Englund M, Kvarnheden A, Johanson U, et al. (2003) The *DAL10* gene from Norway spruce (*Picea abies*) belongs to a potentially gymnosperm-specific subclass of *MADS-box* genes and is specifically active in seed cones and pollen cones. Evol Dev **5**: 551–561

Carlsbecker A, Tandre K, Johanson U, Englund M, Engström P (2004) The MADS-box gene *DAL1* is a potential mediator of the juvenile-to-adult transition in Norway spruce (*Picea abies*). Plant J **40**: 546–557.

Chalupka W and Cecich RA (1997) Control of the first flowering in forest trees. Scand J For Res **12**: 102–111

Cheadle C, Vawter MP, Freed WJ, Becker KG (2003) Analysis of microarray data using Z score transformation. J Mol Diagn **5**: 73

Chen F, Zhang X, Liu X, Zhang L (2017) Evolutionary analysis of MIKCc-Type *MADS-Box* genes in gymnosperms and angiosperms. Front Plant Sci **8**: 895

Chuck GS, Tobias C, Sun L, Kraemer F, Li C, Dibble D (2011) Overexpression of the maize Corngrass1 microRNA prevents flowering, improves digestibility, and increases starch content of switchgrass. Proc Natl Acad Sci USA **42**: 17550–17555

Clough SJ, Bent AF (1998) Floral dip: a simplified method for Agrobacterium-mediated transformation of *Arabidopsis thaliana*. Plant J **16**: 735–743

Curaba J, Talbot M, Li Z, Helliwell C (2013) Over-expression of microrna171 affects phase transitions and floral meristem determinancy in barley. BMC Plant Biol **13**: 6

Dreni L, Zhang D (2016) Flower development: the evolutionary history and functions of the *AGL6* subfamily *MADS-box* genes. J Exp Bot **67**: 1625–1638

Duan Y, Xing Z, Diao Z, Xu W, Li S, Du X, et al. (2012) Characterization of Osmads6-5, a null allele, reveals that *OsMADS6* is a critical regulator for early flower development in rice (Oryza sativa L.). Plant Mol Biol **80**: 429–442

Fan T, Li X, Wu Y, Xia K, Ouyang J, Zhang M, et al. (2015) Rice Osa-miR171c mediates phase change from vegetative to reproductive development and shoot apical meristem maintenance by repressing four OsHAM transcription factors. PLos One **10**: e0125833

Fang J, Chai Z, Yao W, Chen B, Zhang M (2021) Interactions between ScNAC23 and ScGAI regulate GA-mediated flowering and senescence in sugarcane. Plant Sci **304**: 110806

García-López M, C, Vidoy I, Jiménez-Ruiz J, Muñoz-Mérida A, Fernández-Ocaña A, de la Rosa R, et al. (2014) Genetic changes involved in the juvenile-to-adult transition in the shoot apex of *Olea europaea* L. occur years before the first flowering. Tree Genet Genomes **10**: 585–603

George EF, Hall MA, De Klerk G, editors (2008) Stock plant physiological factors affecting growth and morphogenesis. *In* Plant Propagation by Tissue Culture, Ed 3, Springer, Dordrecht, pp 205–226

Gibbons J (2014) Western blot: Protein transfer overview. N Am J Med Sci **6**: 158–59

Guo A, Zhu Q, Gu X, Ge S, Yang J, Luo J (2008) Genome-wide identification and evolutionary analysis of the plant specific SBP-box transcription factor family. Gene **418**: 1–8

Ning G, Yan X, Chen H, Dong R, Zhang W, Ruan Y, et al. (2020) Genetic manipulation of *Soc1-like* genes promotes photosynthesis in flowers and leaves and enhances plant tolerance to high temperature. Plant Biotechnol J **19**: 8–10

Hartmann HT, Kester DE, Davies FTJr,Geneve RL (1997) Plant propagation: principles and practices. Am Midl Nat **63**: 253

Helliwell CA, Wood CC, Robertson M, James Peacock W, Dennis ES (2006) The Arabidopsis FLC protein interacts directlyin vivo with *SOC1* and *FT* chromatin and is part of a high-molecular-weight protein complex. Plant J **46**: 183–192

Böhlenius H (2006) CO/FT regulatory module controls timing of flowering and seasonal growth cessation in trees. Science **312**: 1040–1043

Hepworth SR, Valverde F, Ravenscroft D, Mouradov A, Coupland G (2002) Antagonistic regulation of flowering-time gene *SOC1* by *CONSTANS* and *FLC* via separate promoter motifs. Embo J **21**: 4327–4337

Holefors A, Opseth L, Ree Rosnes A, K, Ripel L, Snipen L, Fossdal G, et al. (2009) Identification of *PaCOL1* and *PaCOL2*, two *CONSTANS-like* genes showing decreased transcript levels preceding short day induced growth cessation in Norway spruce. Plant Physiol Biochem **47**: 105–115

Horvath P (2008) WGCNA: an R package for weighted correlation network analysis. BMC Bioinformatics **9**: 559

Hsu HF, Huang CH, Chou LT, Yang CH (2003) Ectopic expression of an orchid (*Oncidium Gower* Ramsey) *AGL6-like* gene promotes flowering by activating flowering time genes in Arabidopsis thaliana. Plant Cell Physiol **44**: 783–794

Hsu W, Yeh T, Huang K, Li J, Chen H, Yang C (2014) *AGAMOUS-LIKE13*, a putative ancestor for the E functional genes, specifies male and female gametophyte morphogenesis. Plant J **77**: 1–15

Immink RGH, Gadella TWJ, Ferrario S, Busscher M, Angenent GC (2002) Analysis of Mads-box protein-protein interactions in living plant cells. Proc Natl Acad Sci USA **99**: 2416–2421

Jung J-H, Ju Y, Pil J, et al. (2012) The SOC1-SPL module integrates photoperiod and gibberellic acid signals to control flowering time in *Arabidopsis*. Plant J **69**: 577–588

Jungeun L (2010) Regulation and function of SOC1, a flowering pathway integrator. J Exp Bot **61**: 2247–2254

Katahata S, Futamura N, Igasaki T, Shinohara K (2014) Functional analysis of *SOC1-like* and *AGL6-like MADS-box* genes of the gymnosperm Cryptomeria japonica. Tree Genet Genomes **10**: 317–327

Katoh K, Standley DM (2013) MAFFT multiple sequence alignment software version 7: improvements in performance and usability. Mol Biol Evol **30**: 772–780

Khan MRG, Ai X, Zhang J (2014) Genetic regulation of flowering time in annual and perennial plants. RNA **5**: 347–359

Koo SC, Bracko O, Park MS, Schwab R, Chun HJ, Park KM, et al. (2010) Control of lateral organ development and flowering time by the *Arabidopsis thaliana MADS-box* Gene *AGAMOUS-LIKE6*. Plant J **62**: 807–816

Koornneef M, Hanhart CJ, Veen VDJH (1991) A genetic and physiological analysis of late flowering mutants in *Arabidopsis thaliana*. Mol Gen Genet **229**: 57–66

Lauter N, Kampani A, Carlson S, Goebel M, Moose S (2005) microRNA172 down-regulates glossy15 to promote vegetative phase change in maize. Proc Natl Acad Sci USA **26**: 9412–9417

Lee H, Suh SS, Park E, Cho E, Ahn JH, Kim SG, et al. (2000) The AGAMOUS-LIKE 20 MADS domain protein integrates floral inductive pathways in *Arabidopsis*. Genes Dev **14**: 2366–2376

Li H, Liang W, Jia R, Yin C, Zong J, Kong H, et al. (2010) The *AGL6-like* gene *OsMADS6* regulates floral organ and meristem identities in rice. Cell Res **20**: 299–313

Liao S, Cui K, Wan Y, Zhou Z, Li Z, Cui Y, Zhang P, (2014) Reproductive biology of the endangered cypress *Calocedrus macrolepis*. Nord J Bot **32**: 98–105

Liu S, Ma J, Liu H, Guo Y, Li W, Niu S (2020) An efficient system for Agrobacterium-mediated transient transformation in Pinus tabuliformis. Plant Methods **16**: 52

Ma J, Deng S, Chen L, Jia Z, Sang Z, Zhu Z, et al. (2019) Gene duplication led to divergence of expression patterns, protein-protein interaction patterns and floral development functions of *AGL6-like* genes in the basal angiosperm *Magnolia wufengensis* (Magnoliaceae). Tree Physiol **39**: 861–876

Mandel MA, Yanofsky MF (1995) A gene triggering flower formation in *Arabidopsis*. Nature **377**: 522–524

Moon J, Suh S, Lee H, Choi K, Hong CB, Paek N, et al. (2003) The *SOC1 MADS-box* gene integrates vernalization and gibberellin signals for flowering in *Arabidopsis*. Plant J **35**: 613–623

Moyroud E, Kusters E, Monniaux M, Koes R, Parcy F (2010) LEAFY blossoms. Trends Plant Sci **15**: 346–352

Nie J, Stewart H, Zhang JA, Thomson F, Ruan X, Cui , Wei H (2011). TF-Cluster: a pipeline for identifying functionally coordinated transcription factors via network decomposition of the shared coexpression connectivity matrix (SCCM). BMC Syst Biol **5**: 53

Nilsson O, Brunner AM (2004) Revisiting tree maturation and floral initiation in the poplar functional genomics era. New Phytol **164**: 43–51

Nilsson L, Carlsbecker A, Sundås-Larsson A, Vahala T (2007) *APETALA2* like genes from *Picea abies* show functional similarities to their *Arabidopsis* homologues. Planta **225**: 589–602

Nilsson O (2009) Plant evolution: measuring the length of the day. Curr Biol **19**: R302–R303

Niu SH, Liu SW, Ma JJ, Han FX, Li Y, Li W (2019) The transcriptional activity of a temperature-sensitive transcription factor module is associated with pollen shedding time in pine. Tree Physiol **39**: 1173–1186

Niu S, Huwei Y, Xinrui S, Ilga PYL, Yousry A (2016) A transcriptomics investigation into pine reproductive organ development. New Phytol **209**: 1278–1289

Niu S, Li Z, Yuan H, Chen X, Li Y, Li W (2013) Transcriptome characterization of *Pinus tabuliformis* and evolution of genes in the *Pinus* phylogeny. BMC Genomics **14**: 263

Niu S, Liu C, Yuan H, Li P, Li Y, Li W (2015) Identification and expression profiles of sRNAs and their biogenesis and action-related genes in male and female cones of Pinus tabuliformis. BMC Genomics **16**: 693

Nystedt B, Street NR, Wetterbom A, Zuccolo A, Lin Y, Scofield DG, et al. (2013) The Norway spruce genome sequence and conifer genome evolution. Nature **497**: 579–584

Pimentel H, Bray NL, Puente S, Melsted P, Pachter L (2017) Differential analysis of RNA-seq incorporating quantification uncertainty. Nat Methods **14**: 687–690

Poethig RS (2013) Vegetative phase change and shoot maturation in plants. Curr Top Dev Biol **105**: 125–152

Priyanka M, Kishore CP (2015) GIGANTEA—an emerging story. Front Plant Sci **6**: 8

Reinheimer R, Kellogg EA (2009) Evolution of *AGL6-like MADS-box* genes in Grasses (Poaceae): ovule expression is ancient and palea expression is new. Plant Cell **21**: 2591–2605

Rijpkema A S, Zethof J, Gerats T, Vandenbussche M (2009) The petunia *AGL6* gene has a SEPALLATA-like function in floral patterning. Plant J **60**: 1–9

Roberts K, Shirsat AH (2006). Increased extensin levels in *Arabidopsis* affect inflorescence stem thickening and height. J Exp Bot **57**: 537–545

Samach A (2000) Distinct roles of *CONSTANS* target genes in reproductive development of *Arabidopsis*. Science **288**: 1613–1616

Shen G, Yang C, Shen C, Huang K (2019) Origination and selection of ABCDE and AGL6 subfamily *MADS-box* genes in gymnosperms and angiosperms. Biol Res **52**: 25

Shigyo M, Hasebe M, Ito M (2006) Molecular evolution of the *AP2* subfamily. Gene **366**: 256–265

Shim JS, Kubota A, Imaizumi T (2017) Circadian clock and photoperiodic flowering in *Arabidopsis*: *CONSTANS* is a hub for signal integration. Plant Physiol **173**: 5–15

Sohpal VK, Dey A, Singh A (2010) MEGA biocentric software for sequence and phylogenetic analysis: a review. Int J Bioinform Res Appl **6**: 230–240

Tandre K, Albert V A, Sundas A, Engstrom P (1995) Conifer homologues to genes that control floral development in angiosperms. Plant Mol Biol **27**: 69–78

Tandre K, Svenson M, Svensson ME, Engstrom P (1998) Conservation of gene structure and activity in the regulation of reproductive organ development of conifers and angiosperms. Plant J **15**: 615–623

Tapia-Lopez R, Garcia-Ponce B, Dubrovsky JG, Garay-Arroyo A, Perez-Ruiz RV, Kim SH, et al. (2008) An *AGAMOUS-related MADS-box* gene, *XAL1* (*AGL12*), regulates root meristem cell proliferation and flowering transition in *Arabidopsis*. Plant Physiol **146**: 1182–1192

Thompson B E, Bartling L, Whipple C, Hall DH, Sakai H, Schmidt R, et al. (2009) *bearded-ear* encodes a MADS-box transcription factor critical for maize floral development. Plant Cell **21**: 2578–2590

Uddenberg D, Reimegård J, Clapham D, Almqvist C, von Arnold S, Emanuelsson O, et al. (2013) Early cone setting in *Picea abies acrocona* is associated with increased transcriptional activity of a MADS-box transcription factor. Plant Physiol **161**: 813–823

Walden AR, Wang DY, Walter C, Gardner RC (1998) A large family of TM3 MADS-box cDNAs in *Pinus radiata* includes two members with deletions of the conserved K domain. Plant Sci **138**: 167–176

Wang JW, Czech B, Weigel D (2009) miR156-Regulated SPL transcription factors define an endogenous flowering pathway in *Arabidopsis thaliana*. Cell **138**: 738–749

Wang JW, Park MY, Wang LJ, Koo Y, Chen XY, Weigel D, et al. (2011) miRNA control of vegetative phase change in trees. Plos Genet **7**: e1002012

Winter KU, Becker A, Munster T, Kim JT, Saedler H, Theissen G (1999) *MADS-box* genes reveal that gnetophytes are more closely related to conifers than to flowering plants. Proc Natl Acad Sci USA **96**: 7342–7347

Wu F, Shen S, Lee L, Lee S, Chan M, Lin C (2009) Tape-Arabidopsis Sandwich—a simpler *Arabidopsis* protoplast isolation method. Plant Methods **5**: 16

Wu G (2006) Temporal regulation of shoot development in *Arabidopsis thaliana* by miR156 and its target *SPL3*. Development **133**: 3539–3547

Wu G, Park MY, Conway SR, Wang J, Weigel D, Poethig RS (2009) The sequential action of miR156 and miR172 regulates developmental timing in *Arabidopsis*. Cell **138**: 750–759

Xiang W, Li W, Zhang S, Qi L (2019) Transcriptome-wide analysis to dissect the transcription factors orchestrating the phase change from vegetative to reproductive development in *Larix kaempferi*. Tree Genet Genomes **15**:68

Xie K (2006) Genomic organization, differential expression, and interaction of SQUAMOSA promoter-binding-like transcription factors and microRNA156 in rice. Plant Physiol **142**: 280–293

Xu M, Hu T, Zhao J, Park M-Y, Earley KW, Wu G, Yang L, Poethig RS, (2016) Developmental functions of miR156-regulated squamosa promoter binding protein-like (SPL) genes in *Arabidopsis thaliana*. Plos Genet **12**: e1006263

Yan J, Mao D, Liu X, Wang L, Xu F, Wang G, et al. (2017) Isolation and functional characterization of a circadian-regulated *CONSTANS* homolog (*GbCO*) from *Ginkgo biloba*. Plant Cell Rep **36**: 1387–1399

Yano M, Kojima S, Takahashi Y, Lin H, Sasaki T (2001) Genetic control of flowering time in rice, a short-day plant. Plant Physiol **127**: 1425–1429

Yant L, Mathieu J, Dinh TT, Ott F, Lanz C, Wollmann H, et al. (2010) Orchestration of the floral transition and floral development in *Arabidopsis* by the bifunctional transcription factor *APETALA2*. Plant Cell **22**: 2156–2170

Yoo SK, Chung KS, Kim J, Lee JH, Hong SM, Yoo SJ, et al. (2005) CONSTANS activates *SUPPRESSOR OF OVEREXPRESSION OF CONSTANS1* through *FLOWERING LOCUS T* to promote flowering in *Arabidopsis*. Plant Physiol **139**: 770–778

Yoo SK, Wu X, Lee JS, Ahn JH (2011) *AGAMOUS-LIKE 6* is a floral promoter that negatively regulates the *FLC/MAF* clade genes and positively regulates *FT* in *Arabidopsis*. Plant J **65**: 62–76

Zhang B, Horvath S (2005) A general framework for weighted gene co-expression network analysis. Stat Appl Genet Mol Biol **4**: e17

Zhang M, Chen Y, Jin X, Cai Y, Yuan Y, Fu C, et al. (2019) New different origins and evolutionary processes of AP2/EREBP transcription factors in Taxus chinensis. BMC Plant Biol **19**: 413

Zhang Q, Li J, Sang Y, Xing S, Wu Q, Liu X (2015) Identification and characterization of microRNAs in *Ginkgo biloba* var. epiphylla Mak. Plos One **10**: e127184

Zhang Y, Cao G, Qu LJ, Gu H (2009) Characterization of *Arabidopsis* MYB transcription factor gene *AtMYB17* and its possible regulation by *LEAFY* and *AGL15*. J Genet Genomics **36**: 99–107

Wang Z, Shen Y, Yang X, Pan Q, Ma G, Bao M (2019) Overexpression of particular MADS-Box transcription factors in heat stressed plants induces chloroplast biogenesis in petals: chloroplasts biogenesis in petals. Plant Cell Environ **42**: 1545–1560

Zhu Q, Helliwell CA (2011) Regulation of flowering time and floral patterning by miR172. J Exp Bot **62**: 487–495